Front speed in reactive compressible stirred media

Federico Bianco
Institut D'Alembert, University Pierre et Marie Curie, 4 place Jussieu, 75252 Paris Cedex 5, France, CNRS UMR 7190, 4 place Jussieu, 75252 Paris, Cedex 5, France, and Dipartimento di Fisica, Università "La Sapienza," Piazzale Aldo Moro 2, 00185 Rome, Italy

Sergio Chibbaro
Institut D'Alembert, University Pierre et Marie Curie, 4 place Jussieu, 75252 Paris Cedex 5, France and CNRS UMR 7190, 4 place Jussieu, 75252 Paris Cedex 5, France

Davide Vergni
Istituto Applicazioni Calcolo, CNR, Viale Manzoni 30, 00185 Rome, Italy

Angelo Vulpiani
Dipartimento di Fisica, Università "La Sapienza" and ISC-CNR, Piazzale Aldo Moro 2, I-00185 Rome, Italy
(Received 21 January 2013; published 29 April 2013)

We investigated a nonlinear advection-diffusion-reaction equation for a passive scalar field. The purpose is to understand how the compressibility can affect the front dynamics and the bulk burning rate. We study two classes of flows: periodic shear flow and cellular flow, analyzing the system by varying the extent of compressibility and the reaction rate. We find that the bulk burning rate v_f in a shear flow increases with compressibility intensity ϵ, following the relation $\Delta v_f \sim \epsilon^2$. Furthermore, the faster the reaction is, the more important the difference is with respect to the laminar case. The effect has been quantitatively measured, and it turns out to be generally small. For the cellular flow, two extreme cases have been investigated, with the whole perturbation situated either in the center of the vortex or in the periphery. The dependence in this case does not show a monotonic scaling with different behavior in the two cases. The enhancing remains modest and is always less than 20%.

DOI: 10.1103/PhysRevE.87.042924 PACS number(s): 89.75.Kd, 47.70.Fw, 47.70.Pq

I. INTRODUCTION

The dynamics of reacting species presents several issues of great interest from a theoretical point of view [1–3]. Moreover it is also a problem of wide application in many fields, including front propagation in gases [4], chemical reaction in liquids [5,6], and ecological dynamics of biological systems (e.g., plankton in oceans) [7–11].

In the most simplest model of reaction dynamics, the state of the system is described by a single scalar field $\theta(\mathbf{r},t)$ that represents the concentration of products. The field θ vanishes in the regions filled with fresh material (the unstable phase), equals unity where only inert products are left (the stable phase), and takes intermediate values wherever reactants and products coexist, i.e., in the region where production takes place. In their seminal contributions, Fisher, Kolmogorov, Petrovskii, and Piskunov (FKPP) [12,13] considered the simplest case of pure reaction and diffusion and proposed the so-called FKPP model,

$$\partial_t \theta = D\Delta\theta + f(\theta), \tag{1.1}$$

where D is the molecular diffusivity and $f(\theta)$ describes the reaction process that obviously depends on the phenomenon under investigation. In this work, as in the original works of FKPP, we focus on the pulled reaction, e.g., the autocatalytic reaction $f = \alpha\theta(1-\theta)$, where α is the reaction rate and its inverse, $\tau = 1/\alpha$, is the reaction time.

However, most natural phenomena take place in deformable media like fluids, and therefore transport properties cannot be ignored. If the medium is stirred, e.g., a Eulerian velocity field $\mathbf{u}(\mathbf{x})$ is present, Eq. (1.1) can be generalized in the incompressible case to

$$\partial_t \theta + (\mathbf{u}\cdot\nabla)\theta = D\Delta\theta + f(\theta). \tag{1.2}$$

The complete mathematical description of these phenomena is given by partial differential equations (PDE) for the coupled evolution of the velocity field and of the concentration of the reacting species [4]. Therefore Eq. (1.2) should be coupled with Navier-Stokes equations (usually in a nontrivial way). This is the general framework for treating engineering combustion problems in gases [14–16]. In some cases (e.g., [17]), the coupling can be simplified using a Boussinesq term.

In this work, as a further simplification, we assume that the reactants do not influence the velocity field, which evolves independently. In such a limit the dynamics is still nontrivial, and it is completely described by the advection-reaction-diffusion (ARD) Eq. (1.2) together with the proper definition of a given velocity field $\mathbf{u}(\mathbf{x})$. This equation has been intensively studied in incompressible media [18–21]. In particular, the dependence of the front speed as a function of D,α and the velocity field $\mathbf{u}(\mathbf{x})$ [22] has been investigated.

On the contrary, in the case of compressible flows, the ARD problem did not receive very much attention and has only recently been discussed in a mathematical framework [23, 24]. Accounting for compressible flows is, indeed, not simple, but it is a relevant issue in combustion [14,16], in plankton dynamics in turbulent flows [25], and also in particle-laden flows, where the particle phase can be highly compressible even in incompressible flows because of inertia [26–28]. While

the passive scalar approximation for reactive species is hardly tenable in gas combustion phenomena, it may be considered appropriate in aqueous or liquid reactions (notably plankton in oceans) and for dilute particle-laden flows. In those cases, it may give some relevant insights for front propagation and can be used as a model for the flame tracking in some limits [29].

Our aim is to investigate the effects of the compressibility on the bulk burning rate of the reaction process by studying the following PDE:

$$\rho\left[\frac{\partial\theta}{\partial t}+u_i\frac{\partial\theta}{\partial x_i}\right]=D_0\frac{\partial^2\theta}{\partial x_i^2}+f(\theta). \tag{1.3}$$

The scalar field θ represents the mass fraction of a single species of a binary mixture, while u_i is the ith component of a given compressible flow, $D_0=\rho D$ is the diffusion coefficient (supposed to be constant), $f(\theta)=\dot{\omega}$ is the rate of production of the chosen species, and ρ is the nonconstant density of the fluid.

This paper is organized as follows: Sec. II is devoted to the presentation of the model and the principal aspects of the numerical computations. In Sec. III we discuss the results for the front propagation in compressible shear flows. Section IV is devoted to the case of compressible cellular flows. Finally, in Sec. V, we present the conclusions.

II. THE MODEL

The PDE model described by Eq. (1.3) can be derived from the equation of conservation of species, which is relevant for combustion dynamics [4,15]. Let us consider two species (namely, A,B) which diffuse and react together while they are passively transported by a compressible flow, where $\rho_A(x,y,t)$ is the mass of species A per unit volume; the conservation of species A gives

$$\frac{\partial\rho_A}{\partial t}+\frac{\partial}{\partial x_i}[\rho_A(u_i+U_{A,i})]=\dot{\omega}_A, \tag{2.1}$$

where u_i is the ith component of the advective flow field, $U_{A,i}$ is the velocity of diffusion of species A, and $\dot{\omega}_A$ is the rate of production.

Define the mass fraction as $Y_k=\rho_k/\rho$, where ρ is the density of the mixture and $k=A,B$. The species conservation can be written in terms of mass fraction as follows:

$$\frac{\partial(\rho Y_k)}{\partial t}+\frac{\partial}{\partial x_i}[\rho Y_k(u_i+U_{k,i})]=\dot{\omega}_k, \tag{2.2}$$

where $Y_A+Y_B=1$. Moreover, if Fick's law is considered, the diffusion velocities can be defined as follows:

$$Y_AU_{A,i}=-Y_BU_{B,i}=-D\frac{\partial Y_A}{\partial x_i}. \tag{2.3}$$

In the following, we assume an autocatalytic irreversible law $A+B\to 2A$:

$$\dot{\omega}_A=\alpha\rho_A\rho_B=\alpha\rho^2Y_AY_B=\alpha\rho^2Y_A(1-Y_A), \tag{2.4}$$

where the constant α controls the speed of reaction and by definition $\dot{\omega}_A=-\dot{\omega}_B$.

Thus, the evolution of the mass fraction of species A is completely described by the following PDE:

$$\rho\left[\frac{\partial\theta}{\partial t}+u_i\frac{\partial\theta}{\partial x_i}\right]=D_0\frac{\partial^2\theta}{\partial x_i^2}+\alpha\rho^2\theta(1-\theta), \tag{2.5}$$

which holds if we neglect the coupling between the conservation of species equation and the conservation of energy equation. That is the case in which the energy released by the reaction is negligible and thus the momentum and energy equations evolve independently. The left hand side of Eq. (2.5) is written in nonconservative form using the continuity equation of the mixture, and the product $\rho D=D_0$ is assumed to be constant (which is quite a reasonable hypothesis [14,15]).

Since we are interested in the front propagation, we consider the following geometry:

$$-\infty<x<\infty,\quad 0\leqslant y\leqslant L. \tag{2.6}$$

For the sake of simplicity we assume periodic boundary conditions in the y direction and $\theta(-\infty,y,t)=1$ (burned material in combustion terminology) and $\theta(\infty,y,t)=0$ (fresh material).

At $t=0$ the initial condition is given by

$$\theta(x,y,t)=\begin{cases}1 & \text{if } x<0,\\ 0 & \text{if } x\geqslant 0.\end{cases} \tag{2.7}$$

Of course different boundary and initial conditions may be interesting. For instance, if one is interested in quenching issues, appropriate initial conditions would pose θ initially localized in a region of size ℓ,

$$\theta(x,y,0)=\begin{cases}1 & \text{if } -\ell/2\leqslant x\leqslant \ell/2,\\ 0 & \text{if } x<-\ell/2 \text{ or } x>\ell/2.\end{cases} \tag{2.8}$$

Equation (2.5) has been solved using an eighth-order central finite difference scheme in space and a fourth-order Runge-Kutta integration in time. The grid size is sufficiently small to guarantee a good representation of the shear across the reacting region, and the convergence of solutions has been verified. To compute accurately the asymptotic mean bulk burning rate, very long integration periods are required. The grid is remapped following the reacting front, and the computational domain is extended upstream and downstream from the reactive zone so that the boundary effects are negligible.

III. COMPRESSIBLE SHEAR FLOW

We investigate the effects of compressibility in a two-dimensional (2D) steady-state shear flow using the velocity field:

$$\bar{u}(x,y)=\left(\frac{U_0\sin\left(\frac{2\pi y}{L}\right)}{1+\epsilon\sin\left(\frac{2\pi x}{\lambda}\right)},0\right). \tag{3.1}$$

Such a choice corresponds to a Kolmogorov flow with amplitude U_0 and wavelength L, perturbed by a steady wave of wavelength λ and magnitude ϵ accounting for the compressibility of the flow. Let us stress that the perturbation is oriented along the direction of the propagation of the reactive front, i.e., the x axis.

In order to satisfy the continuity equation, $\partial_i(\rho u_i) = 0$, it is necessary to impose a spatial dependence on ρ,

$$\rho(x) = \rho_0 \left[1 + \epsilon \sin\left(\frac{2\pi x}{\lambda}\right)\right].$$

Finally, Eq. (2.5) can be written in nondimensional form,

$$\frac{\partial \theta}{\partial t^*} + u_i^* \frac{\partial \theta}{\partial x_i^*} = \frac{1}{\rho^* \mathrm{Pe}} \frac{\partial^2 \theta}{\partial x_i^{*2}} + \rho^* \mathrm{Da}\theta(1-\theta), \qquad (3.2)$$

if we define $\rho^* = \rho/\rho_0$, $x_i^* = x_i/L$, $u_i^* = u_i/U_0$, $t^* = (tU_0)/L$. The adimensional parameters $\mathrm{Pe} = (\rho_0 U_0 L)/D_0$ and $\mathrm{Da} = (L\alpha\rho_0)/U_0$ are the Péclet and the Damköhler numbers, which define the ratio between the diffusive and advective time scale and the ratio between the advective and reactive time scale, respectively.

In the following, we will drop the star notation, and we will solve Eq. (3.2) focusing on regimes at high Péclet numbers $\mathrm{Pe} \gg 1$. Varying the Damköhler number in a range of $\mathrm{Da} \in [1,1000]$, we will quantify the effects of λ and ϵ on the asymptotic value of the bulk burning rate.

The instantaneous bulk burning rate is

$$v_f(t) = \int_0^1 \int_0^{+\infty} \dot{\omega} dx dy = \int_0^1 \int_0^{+\infty} \mathrm{Da}\rho^2\theta(1-\theta) dx dy, \qquad (3.3)$$

while the mean or asymptotic bulk burning rate is defined as the time average of $v_f(t)$ over a sufficiently long interval:

$$v = \frac{1}{T}\int_0^T v_f(t) dt. \qquad (3.4)$$

To shed some light on the role played by λ we first run a simulation in the absence of compressibility for two different Damköhler numbers (slow and fast reactions) and for a fixed Péclet number. We characterize the thicknesses of the reactive front Δ and δ (see Fig. 1 for definition). From Fig. 1, it is clear that the faster the reaction is, the thinner the flame is.

Then we carry out simulations in which the compressibility is fixed ($\epsilon = 0.5$), and we choose λ that are approximately greater, lower, or between the two thicknesses computed in the case of zero compressibility. In Fig. 2 we show how the geometrical aspect of the reactive front changes by varying λ. In the low density zones, the front thickness appears to be broader than in high density zones due to the decrease of the local Péclet and Damköhler numbers ($\mathrm{Pe}_l = \rho\mathrm{Pe}$, $\mathrm{Da}_l = \rho\mathrm{Da}$). Compressibility perturbation wrinkles the front in the small-wavelength limit, whereas for large wavelengths it is only corrugated since the entire reactive-diffusive front is embedded in a wavelength. Nevertheless, even though the front does not appear to be stationary (even in a comoving reference system) and it is noticeably distorted by the presence of compressibility, the mean velocity of propagation v does not change; see Fig. 3. The wavelength of the perturbation controls the frequency and the magnitude of the instantaneous value of the front speed but does not affect the mean value. Since asymptotic propagation is not affected by λ, from now on in all simulations we set $\lambda = 1$.

In order to quantitatively characterize the effect of compressibility, we vary both ϵ and Da, with a fixed Péclet number. For this purpose, it is convenient to define the percentage

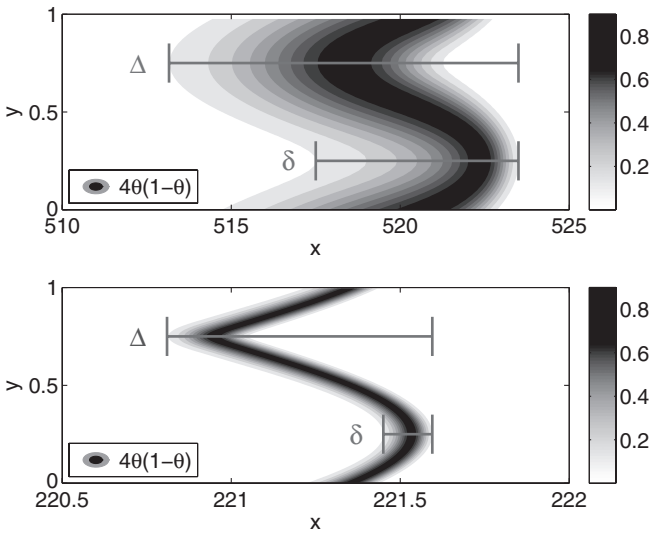

FIG. 1. Shape of the active part of the front [we use the function $4\theta(1-\theta)$, which is maximal for $\theta = 0.5$] for a fixed Péclet number ($\mathrm{Pe} = 100$) and for two different reaction rates. Taking as a reference the incompressible test case ($\epsilon = 0$), we can define two different thicknesses. The bare front thickness is $\delta \sim \sqrt{D/\alpha}$, and the distance between the tip and the tail of the reacting region is Δ. (top) For a slow reaction ($\mathrm{Da} = 1$), we have approximately $\Delta \approx 10$ and $\delta \approx 6$. (bottom) For a fast reaction ($\mathrm{Da} = 100$) $\Delta \approx 0.8$ and $\delta \approx 0.15$.

difference of the mean asymptotic front speed between the compressible and the incompressible cases as follow:

$$\Delta v_{\%} = 100\frac{v - v^0}{v^0}, \qquad (3.5)$$

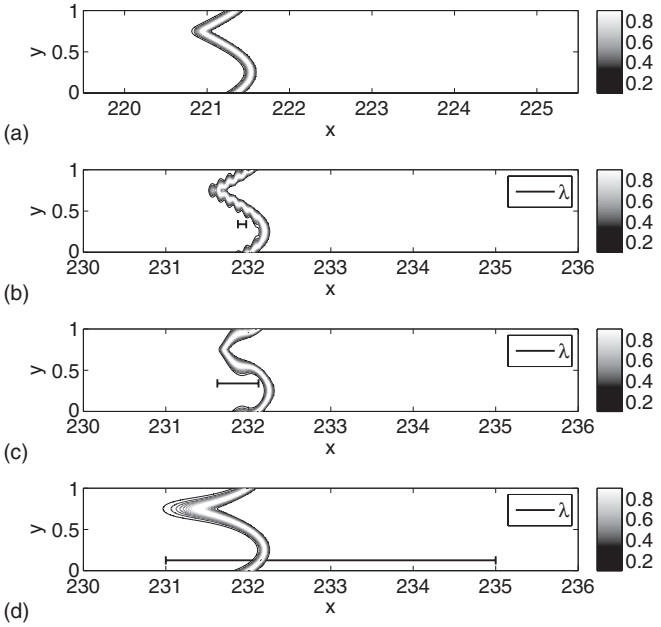

FIG. 2. Snapshot of $4\theta(1-\theta)$ for a fixed Péclet number ($\mathrm{Pe} = 100$) and for Damköhler number $\mathrm{Da} = 100$. (a) An incompressible simulation ($\epsilon = 0$; $\epsilon = 0.5$ in the other panels). For the compressible tests the characteristic length λ is set to be approximately (b) lower ($\lambda = 0.1$), (c) between ($\lambda = 0.5$), or (d) greater ($\lambda = 4$) than the two thicknesses Δ and δ.

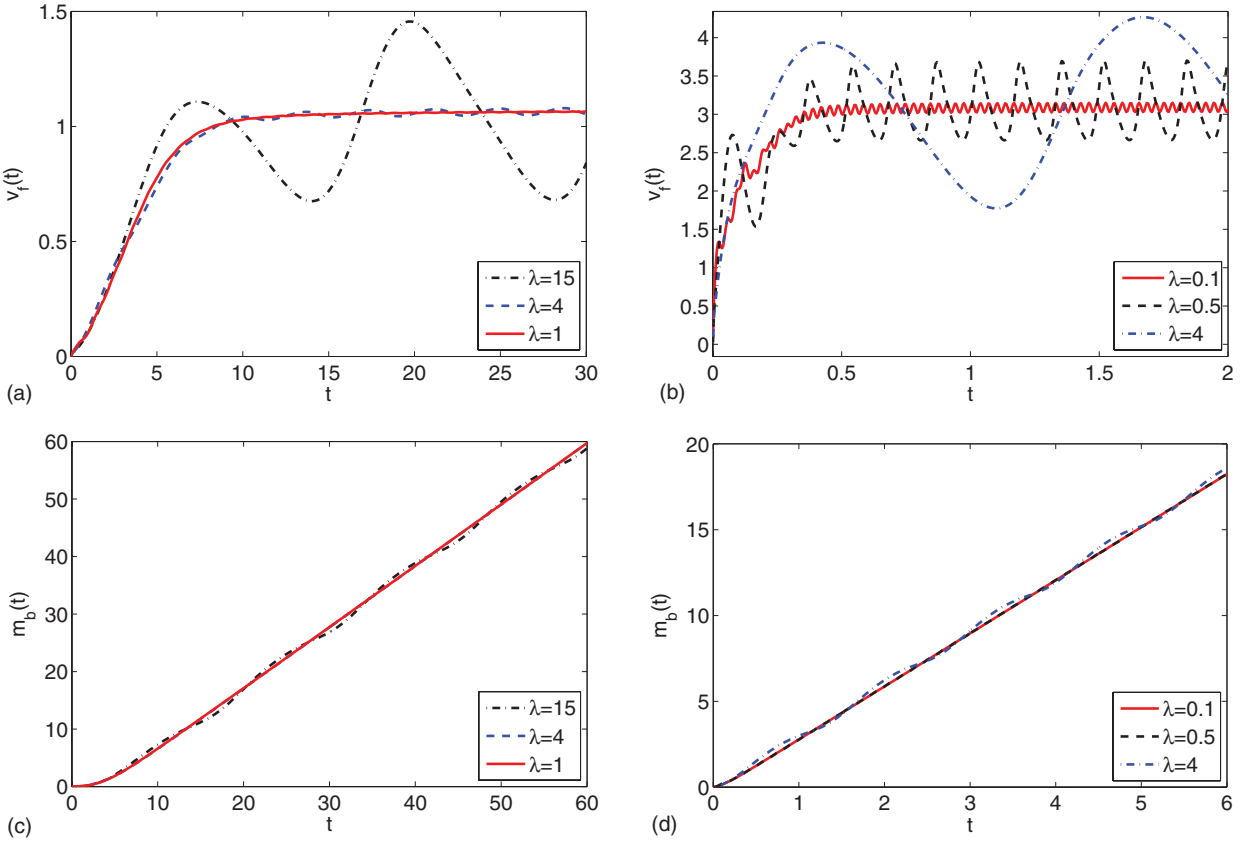

FIG. 3. (Color online) Front speed and burnt mass $[m_b(t) = \int_0^t v_f(t)dt]$ as a function of time for a fixed Pe = 100, two different Damköhler numbers [(a) and (c): Da = 1; (b) and (d): Da = 100], and different λ.

where v^0 is the asymptotic bulk burning rate, as defined in (3.4), for the incompressible case ($\epsilon = 0$). Results are shown in Fig. 4.

In general, in the regimes investigated here, we observe that the presence of compressibility can slightly improve the process of reaction, and the effects grow by increasing both ϵ and Da. For a fixed characteristic reaction rate [see Fig. 4(a)], numerical simulations suggest a power (quadratic) law of the velocity enhancement as a function of parameter ϵ:

$$\Delta v_{\%} \sim \epsilon^2. \tag{3.6}$$

Instead, the dependence on Damköhler number is much slower. As shown in Fig. 4(b), the parameter $\Delta v_{\%}$ is always positive,

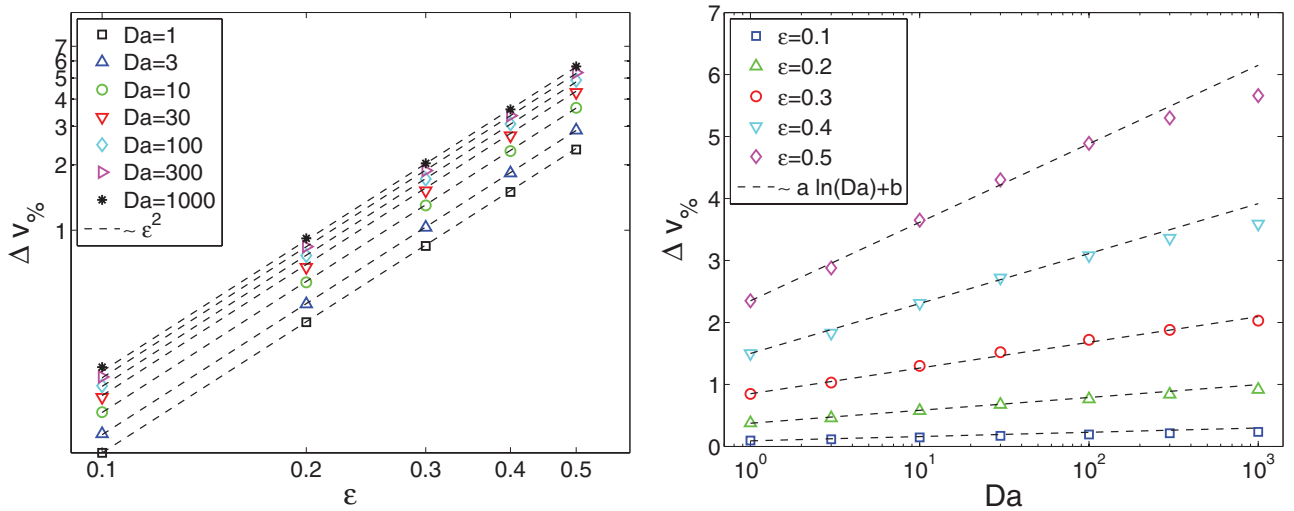

FIG. 4. (Color online) Comparison of the front speed between compressible and incompressible shear flow for a fixed Péclet number (Pe = 100) (left) at different compressibility magnitudes ϵ and (right) for different Damköhler numbers.

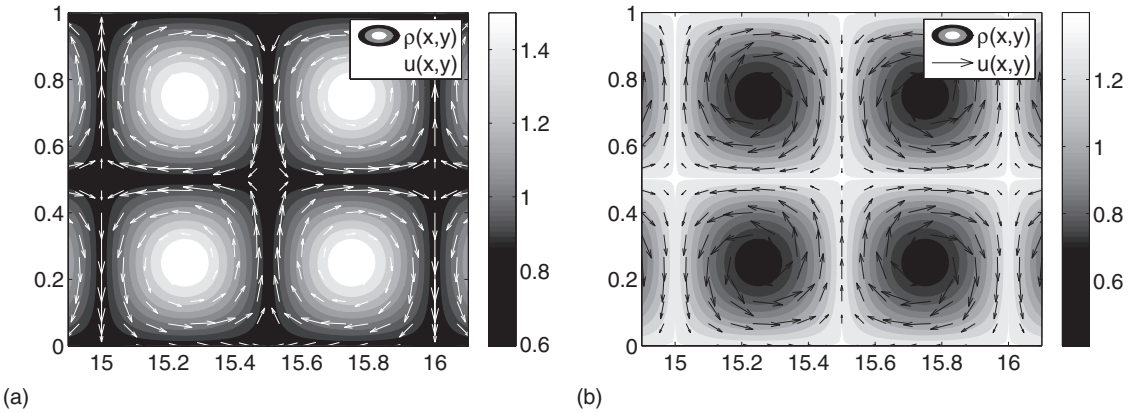

FIG. 5. Compressible Cellular flow : (a) the density is higher in the center of the vortex. (b) The density is higher in the outer region.

and it grows following (approximately) a logarithmic law:

$$\Delta v_{\%} \sim a \ln(Da) + b, \tag{3.7}$$

where a and b may depend on ϵ. Therefore, even in the case of very strong compressibility ($\epsilon = 0.5$) and very fast reaction ($\alpha = 1000$), the difference never exceeds a modest 6%. The effect of compressible wave perturbations appears therefore to be (i) wrinkling and (ii) second-order enhancement.

IV. COMPRESSIBLE CELLULAR FLOW

We discuss now the case of cellular flows, i.e., 2D steady flows of amplitude U_0 composed of a counter-rotating vortex of dimension $L/2$. The compressibility is imposed in the following way:

$$\rho(x,y) = \rho_0 C(x,y), \tag{4.1}$$

$$\vec{u}(x,y) = \left(\frac{U_0 \sin\left(\frac{2\pi y}{L}\right) \cos\left(\frac{2\pi y}{L}\right)}{C(x,y)}, \frac{-U_0 \cos\left(\frac{2\pi y}{L}\right) \sin\left(\frac{2\pi y}{L}\right)}{C(x,y)} \right). \tag{4.2}$$

We choose two different shapes for $C(x,y)$. In the first, which we call case (a), the density of the mixture is higher in the center of the vortex:

$$C(x,y) = 1 + \epsilon \left(\left| \sin\left(\frac{2\pi x}{L}\right) \sin\left(\frac{2\pi y}{L}\right) \right| - \frac{4}{\pi^2} \right). \tag{4.3}$$

In the second, which we call case (b), the density is higher in the periphery of the vortex:

$$C(x,y) = 1 - \epsilon \left(\left| \sin\left(\frac{2\pi x}{L}\right) \sin\left(\frac{2\pi y}{L}\right) \right| - \frac{4}{\pi^2} \right). \tag{4.4}$$

The two different configurations are shown in Fig. 5. The constant factor $\frac{4}{\pi^2}$ has been introduced in order to have a density perturbation which is zero on average. As in the case of the shear flow, we study the dependence of the dynamics on the compressibility intensity ϵ and Damköhler number in the more realistic case of a fixed high Péclet number.

We will consider a wider range of Damköhler numbers, exploring the regimes at $\mathrm{Da} \ll 1$, $\mathrm{Da} \approx 1$, and $\mathrm{Da} \gg 1$. Nevertheless, we will remain in the regime $\mathrm{PeDa} > 1$, which means that the characteristic diffusion time is always larger than the reaction time. Unlike the shear flow, in the cellular flow $\Delta v_{\%}$ does not show a monotonic dependence on either ϵ or Da, as can be seen from Fig. 6.

Such a feature has been observed also for other configurations of $C(x,y)$ (simulations not shown here), confirming

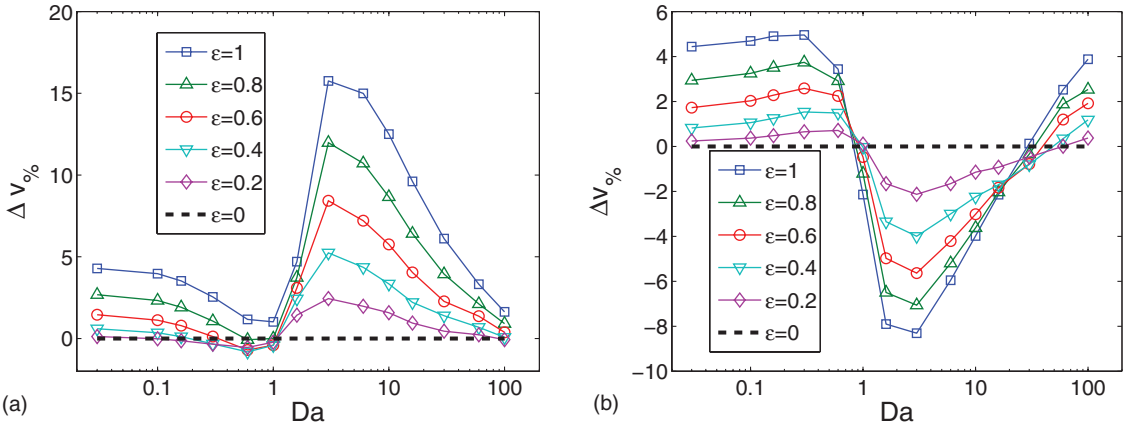

FIG. 6. (Color online) (a) and (b) Percentage difference between compressible and incompressible test cases of the mean asymptotic bulk burning rate. $1/\mathrm{Pe} = 0.003$. In (a) the density of the fluid is higher in the center of the vortices, while in (b) the density is higher in the periphery.

that the nonmonotonic behavior of $\Delta v_{\%}$ is related to the whirling geometry of the flow rather than to the choice of the density perturbation. In the slow reaction regime (Da $\ll 1$) Fig. 6 shows behavior for $\Delta v_{\%}$ that is almost independent of Damköhler number in both cases (a) and (b). On the other hand, in the middle range of the Damköhler number, where the combined effects of advection and reaction are more intriguing, the two flow configurations show opposite trends for $\Delta v_{\%}$; the reaction is faster when the density is higher in the center [case (a)], whereas it is slower when the perturbation is at the periphery [case (b)]. Such a behavior is not surprising since the interplay between reaction and diffusion in the presence of closed streamlines can lead to a nontrivial behavior also in the case of incompressible flow [20], and the presence of variations in the density of the flow can act in a very nonintuitive way.

V. CONCLUSIONS

We have studied the propagation of fronts through an advection-diffusion-reaction equation where the nonlinear reaction term is given by the classical FKPP source term. The advective flow is generated by an imposed field which is perturbed by compressible waves. The compressibility is controlled by the parameter ϵ. Two velocity fields have been considered: a shear flow and a cellular one.

In the considered flows, the front can be strongly affected by compressibility, and the compressibility field forces a strong localization of density, but the quantitative differences with respect to the incompressible model appear to be modest (of the order of some percent). On the basis of previous studies, we do not think that the presence of chaos (turbulent fluctuations) should change the scenario much [21].

Some comments are in order to discuss the apparent difference of the behavior of $\Delta v_{\%}$ in the cases of shear flow and cellular flow (see Figs. 4 and 6). The streamlines in the two cases are very different: namely, open and closed, respectively. In the shear flow, the effect of compressibility on the front propagation is only slightly modified with respect to the incompressible case since the front is mainly driven by the stream. On the other hand, closed streamlines trigger entangled mechanisms between reaction and diffusion that, coupled with the compressibility, generate highly nontrivial features. An example of this complicated behavior can be found in the nonmonotonic dependence of $\Delta v_{\%}$ on the Damköhler number or in the very apparent difference between cases (a) and (b) of the cellular flows considered here.

Finally, it is interesting to note that a similar model has been recently used for the study of population dynamics in turbulent flows [24]:

$$\frac{\partial C}{\partial t} + \nabla \cdot (\mathbf{u}C) = D_0 \nabla^2 C + \mu C(1 - C), \qquad (5.1)$$

where the scalar $C(\mathbf{x},t)$ is the concentration of a population [24], which is the equivalent of $\rho\theta$ in Eq. (2.5). When $\nabla \cdot \mathbf{u} \neq 0$, clustering of the population near compression regions ($\nabla \cdot \mathbf{u} < 0$) is observed. In those regions, the concentration can take values greater than 1, and reaction rate in Eq. (5.1) can be negative, so that the scalar $C(\mathbf{x},t)$ is not a fractional parameter. Within this model, the authors linked changes in the overall carrying capacity of the ecosystem (i.e., the density of biological mass of the system) to the compressibility and its effect of localization. However, the present results show that the change of the carrying capacity is not only due to density localization, but principally to the presence of a reaction term that allows negative rate in high density zones. Indeed, in the present work we have a strong density localization, but our FKPP model for a fractional parameter does not allow a negative rate. The result is that the average carrying capacity does not change even in the presence of compressible flows. The analysis of the present results for the Lagrangian displacement of passive reactive tracers and irreversible reaction dynamics is ongoing.

ACKNOWLEDGMENTS

We would like to thank Dr. Guillaume Legros, P. Perlekar, and Dr. Roger Prud'homme for fruitful discussions.

[1] J. Xin, SIAM Rev. **42**, 161 (2000).
[2] P. Constantin, A. Kiselev, A. Oberman, and L. Ryzhik, Arch. Ration. Mech. Anal. **154**, 53 (2000).
[3] D. Vergni and A. Vulpiani, Milan J. Math. **79**, 497 (2012).
[4] F. A. Williams, *Combustion Theory* (Benjamin-Cummings, Menlo Park, CA, 1985).
[5] J. Ross, S. C. Müller, and C. Vidal, Science **240**, 460 (1988).
[6] I. R. Epstein, Nature (London) **374**, 231 (1995).
[7] E. R. Abraham, Nature (London) **391**, 577 (1998).
[8] E. R. Abraham, C. S. Law, P. W. Boyd, S. J. Lavender, M. T. Maldonado, and A. R. Bowie, Nature (London) **407**, 727 (2000).
[9] J. S. Guasto, R. Rusconi, and R. Stocker, Annu. Rev. Fluid Mech. **44**, 373 (2012).
[10] K. S. Korolev, M. Avlund, O. Hallatschek, and D. R. Nelson, Rev. Mod. Phys. **82**, 1691 (2010).
[11] F. d'Ovidio, S. De Monte, S. Alvain, Y. Dandonneau, and M. Lévy, Proc. Natl. Acad. Sci. USA **107**, 18366 (2010).
[12] A. N. Kolmogorov, I. G. Petrovskii, and N. S. Piskunov, Bull. Moscow Univ. Math. Mech. **1**, 1 (1937).
[13] R. A. Fischer, Ann. Eugenics **7**, 355 (1937).
[14] N. Peters, *Turbulent Combustion* (Cambridge University Press, Cambridge, 2000).
[15] R. Prud'homme, *Flows of Reactive Fluids* (Springer, New York, 2010).
[16] T. Poinsot and D. Veynante, *Theoretical and Numerical Combustion* (Edwards, Philadelphia, 2005).
[17] N. Vladimirova and R. Rosner, Phys. Rev. E **67**, 066305 (2003).
[18] B. Audoly, H. Berestycki, and Y. Pomeau, C. R. Acad. Sci., Ser. IIB, Mech. Phys. Astron. **328**, 255 (2000).
[19] N. Vladimirova, P. Constantin, A. Kiselev, O. Ruchayskiy, and L. Ryzhik, Combust. Theory Modell. **7**, 487 (2003).
[20] M. Abel, M. Cencini, D. Vergni, and A. Vulpiani, Chaos **12**, 481 (2002).

[21] M. Cencini, A. Torcini, D. Vergni, and A. Vulpiani, Phys. Fluids **15**, 679 (2003).
[22] M. Abel, A. Celani, D. Vergni, and A. Vulpiani, Phys. Rev. E **64**, 046307 (2001).
[23] P. Constantin, J. M. Roquejoffre, L. Ryzhik, and N. Vladimirova, Nonlinearity **21**, 221 (2008).
[24] P. Perlekar, R. Benzi, D. R. Nelson, and F. Toschi, Phys. Rev. Lett. **105**, 144501 (2010).
[25] D. M. Lewis and T. J. Pedley, J. Theor. Biol. **205**, 377 (2000).
[26] J. P. Minier and E. Peirano, Phys. Rep. **352**, 1 (2001).
[27] G. Falkovich, K. Gawedzki, and M. Vergassola, Rev. Mod. Phys. **73**, 913 (2001).
[28] J. Bec, L. Biferale, M. Cencini, A. Lanotte, S. Musacchio, and F. Toschi, Phys. Rev. Lett. **98**, 084502 (2007).
[29] N. Vladimirova, V. G. Weirs, and L. Ryzhik, Combust. Theory Modell. **10**, 727 (2006).